Bioorganic & Medicinal Chemistry Letters 19 (2009) 5401–5406

Contents lists available at ScienceDirect

Bioorganic & Medicinal Chemistry Letters

journal homepage: www.elsevier.com/locate/bmcl

Spiropiperidine CCR5 antagonists

David M. Rotstein *, Stephen D. Gabriel, Ferenc Makra, Lubov Filonova, Shelley Gleason, Christine Brotherton-Pleiss, Lina Q. Setti, Alejandra Trejo-Martin, Eun Kyung Lee, Surya Sankuratri, Changhua Ji, Andre deRosier, Marianna Dioszegi, Gabrielle Heilek, Andreas Jekle, Pamela Berry, Paul Weller, Cheng-I. Mau

Roche Palo Alto LLC, 3431 Hillview Avenue, Palo Alto, CA 94304, USA

ARTICLE INFO

Article history:
Received 25 June 2009
Revised 24 July 2009
Accepted 24 July 2009
Available online 30 July 2009

Keywords:
CCR5 antagonist
Chemokine
Anti-HIV-1
Antiviral
Spiropiperidine

ABSTRACT

A novel series of CCR5 antagonists has been identified, utilizing leads from high-throughput screening which were further modified based on insights from competitor molecules. Lead optimization was pursued by balancing opposing trends of metabolic stability and potency. Selective and potent analogs with good pharmacokinetic properties were successfully developed.

The eruption of the AIDS epidemic in the 1980's catalyzed a corresponding huge response from the academic, medical and pharmaceutical communities to identify the responsible pathogen and develop medications to treat this affliction. Notable progress has been made in the intervening decades, however significant challenges remain. The remarkable ability of the virus to rapidly mutate and generate resistant strains necessitates the continued development of new pharmaceuticals, particularly ones which employ novel mechanisms of intervention.[1] The observation that a small percentage of high-risk populations showed either resistance or delayed development of disease led to the discovery of the key role played by the chemokine cell surface co-receptors CCR5 and CXCR4 for successful viral fusion and infection. These discoveries triggered a search for small molecule antagonists which would function as viral entry inhibitors.[2]

A variety of such antagonists have been disclosed and in 2007 the first CCR5 antagonist, Selzentry®, was approved and launched by Pfizer.[3] Development of new, novel CCR5 antagonists continues both for their antiviral effects and also for potential utility in a variety of autoimmune indications.[4] In this publication we describe some of our efforts in this field.

The development of our CCR5 antagonist series combined an information driven approach with leads from high-throughput assays. Screening of the Roche library uncovered a number of low potency hits containing the spiropiperidine template 1-oxa-3,8-diazo-spiro[4,5]decan-2-one, **1**. Researchers at Ono had earlier disclosed a series of spiropiperidine CCR5 antagonists[5] leading to the clinical candidate aplaviroc **2**.[6] As illustrated in Figure 1, combination of our spiropiperidine template **1** with pharmacophore elements from both aplaviroc and from Schering's CCR5 antagonist program[7] (exemplified by **3**), led to analog **4**, the initial lead compound in our series. Indeed, as seen in Table 1, analog **4** showed promising activity in both binding and antiviral assays.[8]

Compound **4** had extremely poor in vitro metabolic stability: intrinsic clearances in human (HLM) and rat (RLM) liver microsomes were 675 and 2000 μL/min/mg protein, respectively,[9] which corresponded to projected in vivo clearances close to hepatic blood flow.[10] Thus, our objective was to improve the drug-like properties of the series while improving antiviral potency.

In describing results from our SAR studies, the benzamide and cyclohexyl groups are typically referred to as the head and tail groups of the template respectively. Initial studies with this series demonstrated that while binding activity was maintained with a variety of structural modifications, antiviral activity was much more sensitive,[11] requiring conservation of all major pharmacophore elements. As seen in Table 1, removal of a flanking methyl group on the benzamide head group **5** led to loss of antiviral activity. Removal or shrinkage of the cyclohexyl tail substituent to cyclopentyl **6** also led to diminished activity. Replacement of the cyclohexyl tail substituent by either heterocyclic or aromatic rings such as pyran **7** or phenyl **8** also led to loss in antiviral potency. The butyl side chain proved

* Corresponding author. Tel.: +1 650 852 1947; fax +1 650 855 6585.
E-mail address: david.rotstein@roche.com (D.M. Rotstein).

0960-894X/$ - see front matter © 2009 Elsevier Ltd. All rights reserved.
doi:10.1016/j.bmcl.2009.07.122

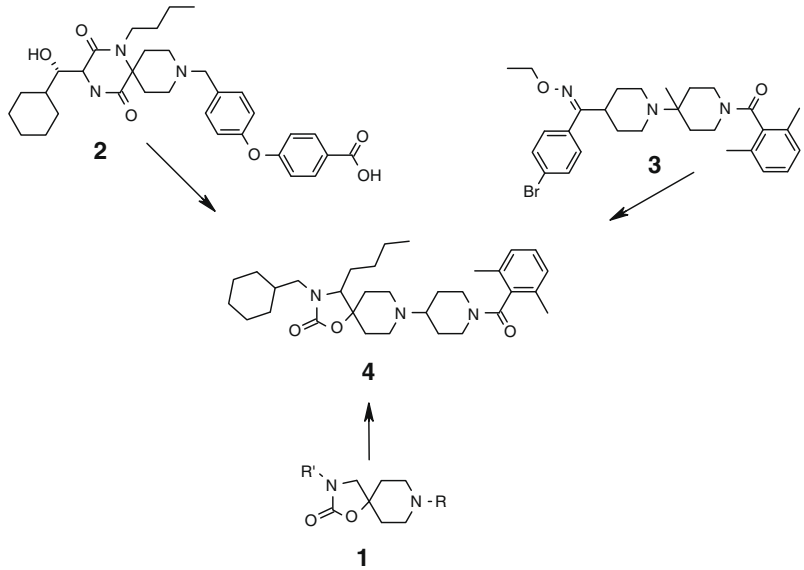

Figure 1.

similarly intolerant to modification as seen by the loss of antiviral activity with propyl side chain analog **9**. Introduction of an angular methyl group (similar to one utilized in Schering's CCR5 template) did improve antiviral potency, as seen with analog **10**. Metabolic stability remained a major issue with this template as exemplified by **10** with human and rat intrinsic microsomal clearance of 526 and 523 μL/min/mg protein, respectively.

Metabolite profiling of our series showed multiple oxidative metabolites, particularly on the lipophilic cyclohexyl tail and phenyl head substituents. To combat this problem, in analogy to Schering's approach[7], a strategy of heteroatom introduction into these groups was pursued to block metabolism and lower overall lipophilicty. As shown in Table 2, replacement of the phenyl head group with pyrimidine afforded analog **11** which demonstrated much improved metabolic stability in human liver microsomes. Further replacement of cyclohexane tail with pyran resulted in metabolically stable analog **12**. Unfortunately, these modifications also resulted in loss of antiviral activity and the emergence of active efflux by P-glycoprotein (P-gp) as an issue.

This example is representative of a common trend observed in our series where reduction of lipophilicity increased metabolic stability but also led to decreased potency and increased efflux by P-gp. Moving forward, our objective was to balance these parameters to achieve the desired profile for a clinical candidate.

A key finding was that expansion of the spiro carbamate from a 5 to a 6 member ring afforded a template which allowed greater opportunity to balance potency and drug-like properties. As shown in Table 3, analog **13**, containing the 1-oxa-3,9-diaza-spiro [5.5]undecane-2-one spiropiperidine template demonstrated impressive antiviral potency, although metabolic stability was still an issue (HLM intrinsic clearance of 307 μL/min/mg). However, unlike the 5 member spiro system, introduction of heteroatoms into the head and tail region was tolerated in the 6 member spiro system without significant loss in potency. This can be seen with analog **14**, where phenyl has been replaced by pyrimidine. Indeed, analog **14** demonstrated improved metabolic stability in both human and rat intrinsic microsomal clearance: 119 and 80 μg/min/mg, respectively. This improved in vitro metabolic stability translated into very promising oral bioavailability in rats: 43% F, at 10 mg/kg. Of concern for this compound was the low projected human exposure due to high metabolic clearance (82% hepatic blood flow). Further efforts targeted improving this parameter.

Introduction of additional heteroatoms into our template to improve metabolic stability and lower lipophilicity was explored next. All modifications of the butyl side chain led to decreased activity, including longer, shorter or cyclic side chains and heteroatom substitution at a variety of positions (data not shown). Introduction of heteroatoms into the tail cyclohexyl group was tolerated as seen in pyran analog **15**. However, as with the 5 member spiro system, combination of a pyran tail with a pyrimidine head group led to loss of antiviral activity, as seen with analog

Table 1
SAR of lead compound **4**

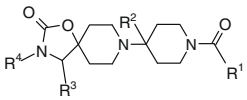

#	R^1	R^2	R^3	R^4	Binding[a] IC_{50}	Antiviral[b] IC_{50}
4		H	*n*Bu		51	125
5		H	*n*Bu		100	>625
6		H	*n*Bu		18	>625
7		H	*n*Bu		24	>625
8		H	*n*Bu		144	>625
9		H	*n*Pr		300	>625
10		Me	*n*Bu		10	<1.2

[a] Competitive binding evaluated vs. RANTES with IC_{50} values in nM, as mean of two experiments.
[b] Antiviral IC_{50} values in nM as mean of two experiments.

Table 2
SAR of the 1-oxa-3,8-diazo-spiro[4,5]decan-2-one template

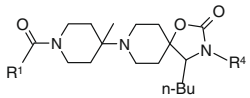

#	R^1	R^4	Binding [a]IC_{50}	Antiviral[a] IC_{50}	clog *P*	HLM[b]	Caco[c] AB/ER
10			10	<1.2	6.4	526	14/0.4
11			7	46	4.4	162	ND[d]
12		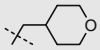	58	375	2	27	0.6/31

[a]Defined as in Table 1[b] human liver microsomal intrinsic clearance (μl/min/mg protein) [c] Permeability in Caco-2 cells AB, apical to basolateral and BA, basolateral to apical movement of test compound in 21 day cultured Caco-2 cells (cm/sec × $10E^{-6}$). ER, efflux ratio of BA to AB [d] not determined.

16. Fortunately, it was found that the introduction of an angular methyl group into the 6 member spiro template restored antiviral potency, even with the incorporation of heteroatoms necessary to enhance metabolic stability. This can be seen with analog **17**, which possesses a promising combination of antiviral potency and microsomal stability.

Compound **17** is a racemate and as shown in Table 4, demonstrated that antiviral activity resided in the (*S*) enantiomer **19**.

As SAR studies on this template progressed, a wide tolerance for substitution was demonstrated. These studies focused on the active (*S*) enantiomers.

Analogs **20–25** show modifications to the head group which maintain good potency, including the pyridine, pyridine, N-oxide, cyanopyridine, pyrone and 2-trifluoromethyl pyrimidine groups. Introduction of the cyanopyridine head group (as in analog **22**), consistently provided excellent antiviral activity across many examples. This can be clearly seen in the case of compound **23**, where despite trimming of the tail group down to only methyl, incorporation of a cyanopyridine head group maintains good antiviral activity. In contrast, all activity is lost when a methyl tail is combined with a pyrimidine head group (data not shown). Unfortunately, metabolic stability decreased with fully elaborated cyanopyridine analogs, as seen with analog **22**. The effect of modification on the tail group was examined next. Lipophilic groups such as difluorocyclohexyl **26** maintain excellent antiviral activity, but with concurrent loss of metabolic stability. Movement of the pyran oxygen around the ring, as in analog **27**, results in a loss of potency, as does removal of the methylene tail linker as shown in **28** which had an antiviral IC_{50} of 84 nM. Extension of the linker to ethyl, **29**, is tolerated, but at a cost of microsomal stability (AV IC_{50} 8 nM, HLM clearance 37 μl/min/mg). Incorporation of aromatic or heteroaromatic groups led to lower potency.

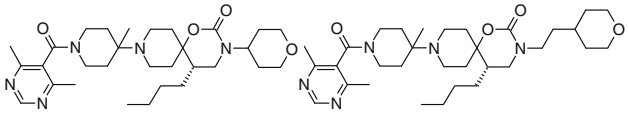

28 **29**

Table 3
SAR of the 1-oxa-3,9-diaza-spiro[5.5]undecane-2-one template

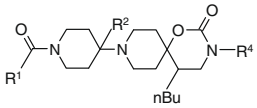

#	R^1	R^2	R^4	Binding IC_{50}[a]	Antiviral IC_{50}[a]	clog *P*	HLM[a]
13		H		30	29	6.5	307
14		H		68	31	4.5	119
15		H		89	24	4.1	164
16		H		76	405	2.1	ND
17		Me		25	14	2.6	17

[a] Defined as in Tables 1 and 2.

Table 4
SAR of the chiral 1-oxa-3,9-diaza-spiro[5.5]undecane-2-one template

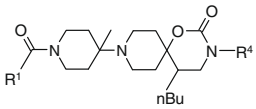

#	R^1	*n*Bu	R^4	Binding IC_{50}[a]	Antiviral IC_{50}[a]	HLM[a]
18		*R*	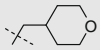	100 (*n* = 1)	>625	17
19		*S*	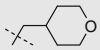	25	6	12
20		*S*	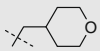	61	4	33
21	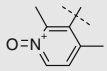	*S*	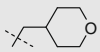	80	52	ND
22	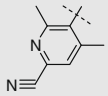	Racemate	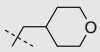	24	4	42
23	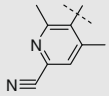	*S*	Me	22	12	28
24		*S*	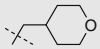	12	3	36
25	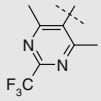	*S*	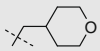	97	3	46
26		*S*	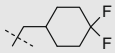	27	2	106
27		*S*		10	55	53

[a] Defined as in Tables 1 and 2.

An analysis of our data pointed to analog **19** as having the most promising profile and subsequent efforts focused on further profiling of this compound. None of the major hepatic cytochrome P450 enzyme isoforms (3A4, 1A2, 2C9, 2C19 and 3D6) were inhibited by analog **19**. Plasma protein binding was moderate across species: the free fraction in rat, dog, monkey and human plasma was 32%, 13%, 4% and 17%, respectively. Table 5 shows the favorable pharmacokinetic data generated for compound **19** in rat,[12] dog and monkey.

Analog **19** proved very selective for the human CCR5 receptor. Screening of **19** for binding versus a panel of other chemokine receptors (CCR1, 2b, 3, 4, 6 and CXCR4) showed no cross reactivity with IC_{50}'s >50 μM. An assessment of in vitro hERG inhibition for **19** at 37 °C gave IC_{50} and IC_{20} values of 11.9 and 2.9 μM, respectively. The biological activity of analog **19** was further assessed by screening in a peripheral blood mononuclear cell (PBMC) viral replication assay with 10% FBS using an R5-tropic HIV-$_{Ba\text{-}L}$ strain. The excellent potency of this compound was confirmed, affording an IC_{50} of 0.18 nM.

The synthesis of analogs **4–12** from the 1-oxa-3,8-diazospiro[4,5]decan-2-one series is outlined in Scheme 1.[13]

Generation of the dianion of hexanoic acid with LDA followed by reaction with 4-oxo-piperidine-1-carboxylic acid benzyl ester **30** gave hydroxy acid **31**. Treatment of **31** with diphenylphospho-

Table 5
Pharmokinetic profile of analog 9[a]

Pharmacokinetics[b]	Rat	Dog	Monkey[c]
C_{max} (ng/mL)	13	225	42
AUC (ng h/mL)	54	700	396
Cl (mL/min/kg)	52	20	19
$T_{1/2}$ (h)	1.4	2.9	3.5
Vd_{ss}(L/kg)	3.8	3.2	3.0
F%	10	85	42

[a] Doses were 1 mg/kg IV and PO for all species.
[b] C_{max}, AUC and %F were determined after the oral dose and Cl, Vd_{ss}, $t_{1/2}$ were determined from the iv dose.
[c] Cynomolgus monkey.

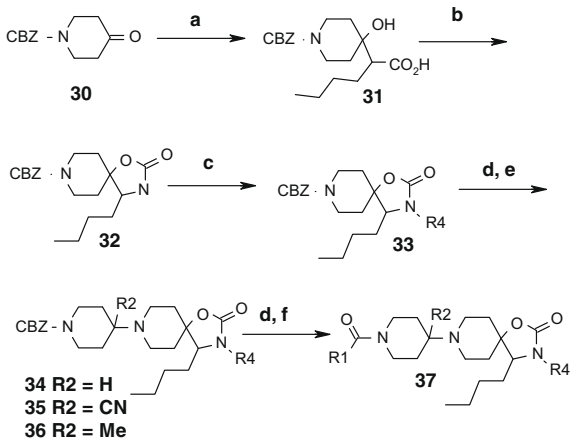

Scheme 1. Reagents and conditions: (a) $CH_3(CH_2)_4CO_2H$, LDA, THF, −78 °C to rt, 99%; (b) $(PhO)_2P(O)N_3$, TEA, toluene, reflux, 75%; (c) R_4Br, NaH, DMF, 70 °C, yield range: 20–85%;(d) 10% Pd/C, H_2·EtOH, rt, 95%; (e) (i) **30**, Ti(*i*-OPr)$_4$, $ClCH_2CH_2Cl$, rt; (ii) NaHB(OAc)$_3$, rt, 56% or (i) **30**, Ti(*i*-OPr)$_4$, Et_2AlCN, THF; (ii) MeMgBr, THF, rt, 61% for two steps; (f) R_1CO_2H, EDCI, HOBT, *i*Pr_2NEt, DMF, rt, yield range: 25–90%.

ryl azide gave the intermediate acyl azide, which upon heating underwent a Curtius rearrangement and subsequent cyclization to afford the spiro system **32**. Alkylation of the carbamate in the presence of sodium hydride provided intermediate **33**. The second piperidine ring was incorporated by a Strecker reaction of the deprotected amine via titanium isoproxide mediated condensation with ketone **30**, followed by sodium triacetoxyborohydride reduction of the intermediate imine to give **34**. Alternatively, treatment of the imine with diethylaluminum cyanide afforded nitrile **35** which can be converted to methyl analog **36** under Bruylant conditions with methyl magnesium bromide. Final amide formation was accomplished by deprotection of **36** followed by treatment with requisite carboxylic acids, HOBT, EDCI and base to give product **37**.

The synthesis of analogs **13–29** from the 1-oxa-3,9-diaza-spiro[5,5]undecan-2-one series is outlined in Scheme 2.[13] The anion from hexanenitrile was generated by treatment with *n*-butyl lithium, then reacted with 1-benzyl-4-oxo-piperidine **38** to afford cyanoalcohol **39**. Nitrile reduction with LAH afforded amino alcohol **40**. Intramolecular cyclization of the amino alcohol with CDI afforded carbamate **41**. In a process analogous to Scheme 1, N-alkylation, deprotection of the piperidinyl nitrogen, amination with N-protected 4-oxo-piperidine, deprotection and amide coupling lead to final product **46**.

The synthetic sequence used to prepare chiral analogs from the 1-oxa-3,9-diaza-spiro[5,5]undecan-2-one series is illustrated in Scheme 3 for the preparation of inhibitor **19**. Wittig olefination of N-Boc piperidone **47** afforded the 4-pentylidene intermediate **48**. Asymmetric dihydroxylation using AD-mix-β afforded chiral diol **49**, which was selectively mesylated on the secondary alcohol, then converted to chiral epoxide **50** upon basic treatment. Epoxide opening with diethylaluminum cyanide afforded hydroxynitrile **51**, which was reduced to amino alcohol **52** under Suzuki reduction conditions with cobalt(II) chloride hexahydrate and sodium borohydride. Cyclic carbamate **53** was then formed by treatment of the amino alcohol with CDI. After BOC removal with TFA, a Strecker reaction, via titanium isopropoxide mediated condensation of the amine with ketone **47** and reaction of the intermediate imine with diethylaluminum cyanide afforded nitrile **54**. Subsequent treatment of **54** under Bruylant conditions with methyl magnesium bromide afforded the methyl analog **55**. Alkylation of **55** with 2-bromomethyl tetrahydropyran and sodium hydride, followed by N-BOC removal with TFA afforded the penultimate intermediate **56**. Final amide formation with 4,6-dimethyl-pyrimidine-5-carboxylic acid using HOBt, EDCI and base gave final product **19**.

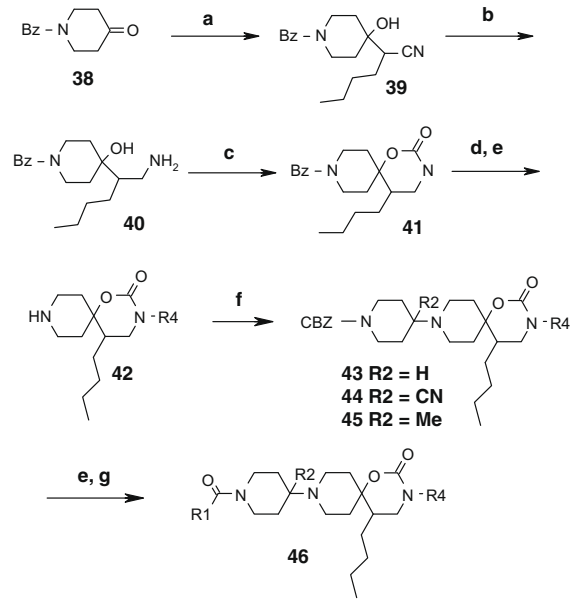

Scheme 2. Reagents and conditions: (a) $CH_3(CH_2)_4CN$, *n*BuLi, THF −78 °C, 53%; (b) LAH, THF, 0 °C; (c) CDI, THF, rt, 62% for two steps; (d) R_4Br, NaH, DMF, yield range: 25–75%; (e) 10% Pd/C, H_2·EtOH, rt, 79%; (f) (i) **30**, Ti(*i*-OPr)$_4$, $ClCH_2CH_2Cl$, rt; (ii) NaHB(OAc)$_3$, rt, 77% for two steps or (i) **30**, Ti(*i*-OPr)$_4$, Et_2AlCN, THF; (ii) MeMgBr, THF, rt, 60% for two steps; (g) R_1CO_2H, EDCI, HOBT, *i*Pr_2NEt, DMF, rt, yield range: 30–85%.

In summary, we have discovered a novel series of potent CCR5 small molecule antagonists, exemplified by analog **19**, possessing good selectivity and pharmacokinetic properties.

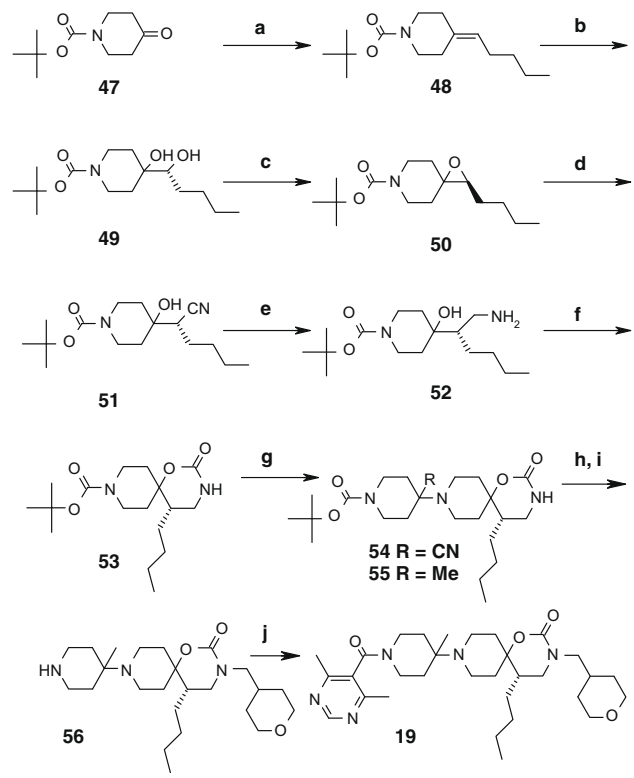

Scheme 3. Reagents and conditions: (a) $CH_3(CH_2)_4PPh_3Br$, *n*BuLi, THF, −78 °C, 36%; (b) AD-mix-β, $CH_3SO_2NH_2$, *t*-BuOH, H_2O, 91%; (c) (i) CH_3SO_2Cl, TEA, EtOAc, CH_2Cl_2,0 °C; (ii) NaOMe, MeOH, 95% for two steps; (d) Et_2AlCN, THF, 0 °C, 58%; (e) $CoCl_2$·$6H_2O$, $NaBH_4$, 86%; (f) CDI, THF, 69%; (g) (i) CF_3CO_2H, CH_2Cl_2; (ii) **47**, Ti(*i*-OPr)$_4$, Et_2AlCN, THF; (iii) MeMgBr, THF, 71% for three steps; (h) 2-bromomethyl tetrahydropyran, NaH, THF, 86%; (i) CF_3CO_2H, CH_2Cl_2; (j) 4,6-dimethylpyrimidine-5-carboxylic acid, EDCI, HOBT, *i*Pr_2NEt, DMF, 92%.

Acknowledgments

The authors thank Rebecca Stephenson, Gary Cooper, Ann Petersen, Fernando Padilla, Chris Melville, Remy Lemoine, Lijing Chen, Jason Manka and David Loughhead for synthetic support; Rama Kondru, Nidhi Arora and Taraneh Mirzadegan for computational support; Yanzhou Liu for expert NMR analysis; Marquis L. Cummings Jr. for chiral HPLC purifications; Naina Patel for formulation development; Joe Muchowski, Counde Oyang, David Goldstein, David Swinney, Denis Kertesz and Eric Sjogren for helpful discussions.

References and notes

1. Wainberg, M. A.; Jeang, K.-T. *BMC Med.* **2008**, *6*, 1.
2. Kuhmann, S. E.; Hartley, O. *Annu. Rev. Pharmacol. Toxicol.* **2008**, *48*, 425.
3. Kuritzkes, D.; Kar, S.; Kirkpatrick, P. *Nat. Rev. Drug Disc.* **2008**, *7*, 15.
4. Turner, J. E.; Steinmetz, O. M.; Stahl, R. A.; Panzer, U. *Mini-Rev. Med. Chem.* **2007**, *7*, 1089.
5. Habashita, H.; Kikubo, M.; Hmano, S.; Hamanaka, N.; Masaaki, T.; Shibayama, S.; Tada, H.; Sagawa, K.; Fukushima, D.; Maeda, K.; Mitsuya, H. *J. Med. Chem.* **2006**, *49*, 4140.
6. McIntyre, J. A.; Castñer, J. *Drugs Future* **2004**, *29*, 677.
7. Palani, A.; Shapiro, S.; Clader, J. W.; Greenlee, W. J.; Cox, K.; Strizki, J.; Endres, M.; Baroudy, B. M. *J. Med. Chem.* **2001**, *44*, 3339.
8. For assay protocols see: Melville, C.R.; Rotstein, D. M. WO2008119663.
9. The thresholds above which intrinsic mircrosomal clearance values were considered to be high were ⩾90 μl/min/mL for RLM and ⩾35 μl/min/mL for HLM. These scaled to in vivo clearance values ⩾70% of liver blood flow using the well-stirred model. Intrinsic microsomal clearance values corresponding to ⩽30% of liver blood flow (⩽15 μl/min/mL for RLM and ⩽6.5 μl/min/mL for HLM) were considered to be low.
10. Obach, R. S. *Curr. Opin. Drug Discovery Dev.* **2001**, *4*, 36.
11. Ernst, J.; Dahl, R.; Lum, C.; Sebo, L.; Urban, J.; Miller, S. G.; Lundström *J. Bioorg. Med. Chem. Lett* **2008**, *18*, 1498.
12. The relatively low exposure observed in rat was due to active transport, in addition to metabolic clearance. Pre-treatment with the P-gp inhibitor elacridar gave higher exposures due to reduced biliary excretion and intestinal secretion. Saturation of transporter effects upon higher dosing also gave improved exposures.
13. For more detailed experimental data, see: Gabriel, S. D.; Rotstein, D. M. US Patent 2005, 176703, Ref. 8.